THE JOURNAL OF PHYSICAL CHEMISTRY B

ARTICLE

pubs.acs.org/JPCB

Measurements of *G* Values for DNA Damage Induced by Low-Energy Electrons

Elahe Alizadeh* and Léon Sanche

Groupe en science des radiations, Département de médecine nucléaire et radiobiologie, Faculté de médecine et des sciences de la santé, Université de Sherbrooke, J1H 5N4 Sherbrooke, Canada

ABSTRACT: We address the problem of measuring *G* values (damage per unit of deposited energy) for low-energy electrons (LEEs) below 30 eV. Such values (G_{LEE}) usually have to be derived from damage yields in nanometer- (∼10-nm-) thick films, which are too thin to allow complete absorption of the energy of LEEs. In this work, we determine optimum corrections to obtain reliable G_{LEE} values in 2−80-nm-thick films of plasmid DNA that are not uniform. G_{LEE} was found to increase with average film thickness and reach a plateau at 260 ± 50 nmol/J around 20 nm, which corresponds to the most reliable value. The previously measured G_{LEE} values for films thinner than 20 nm that were underestimated can be corrected using a factor derived from the present results. This method could be used to obtain reliable G_{LEE} values for other biomolecules so as to enable the comparison of LEE-induced damage to that produced by other types of radiation under various experimental conditions.

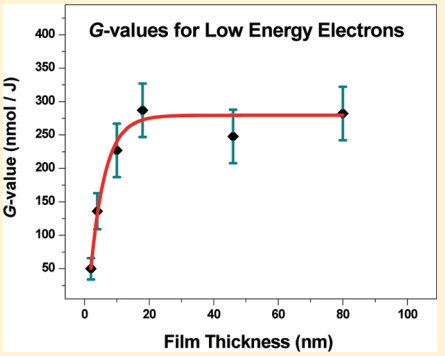

1. INTRODUCTION

Cell killing by ionizing radiation is associated with structural damage to cellular DNA through the formation of lesions such as strand breaks, base modifications, and cross-links.[1−3] For this reason, radiation physics and chemistry studies have attempted to link biological damage to fundamental processes including the production of electrons, ions, electronic excited states,[4−6] and subsequent reactions.[1,6−11] Many studies have involved reactions of radiation products in aqueous solutions with DNA molecules.[1,6−9] To compare the yields of damage in the different experimental models, radiation chemists measure a universal quantity referred to as the *G* value. Thus, the damage imparted for high-energy radiation is often quantified by measuring the *G* value, which corresponds to the number of moles of substance produced per joule of radiation energy absorbed.[12] The *G* value depends not only on the target, but also on the energy and type of radiation. Most of these *G*-value measurements have been performed with high-energy radiation under different experimental conditions. For example, the *G* values for single strand breaks (SSBs) induced in DNA have been measured at various energies for X- and γ-rays,[12,13] α-particles,[14,15] and high-energy electrons.[16]

With high-energy particles or photons, measurements of *G* values usually do not pose any particular problem because macroscopic or at least sufficiently thick targets are irradiated. With such targets, the amount of energy deposited can simply be obtained from the attenuation coefficient of the absorbing matter, because in this case, the product of the number of attenuated particles with the energy of the particles is equal to the energy absorbed. However, for nanoscale-thin targets, this condition is usually not met; that is, not all of the energy of the scattered photons or particles is deposited in the sample, so that the measured *G* values are underestimated. In present work, we address this problem in the case of *G*-value measurements for DNA damage induced by low-energy electrons (LEEs).

DNA damage induced by LEEs has been extensively investigated in the past decade to understand the basic mechanisms affecting the induction of biological lesions.[3,17,18] Such electrons with initial kinetic energies below 30 eV are produced in large quantities[19] and play a central role in propagating the effects of ionizing radiation.[6,17] LEEs have thermalization distances on the order of 10 nm in biological materials, which define the initial volume of energy deposition.[4,20] This range is comparable to the diameter of DNA (2−5 nm) and the nucleosome (10 nm).[5] This property of LEEs requires that one work with targets that are as thin and as uniform as possible to avoid charging by thermalized electrons. LEE experiments are therefore usually performed with films of DNA or other biomolecules condensed or deposited on a metal substrate.[3,21] The film thickness is usually less than the thermalization distance of the LEEs. To date, a fairly large number of experiments have measured the damage induced in DNA by LEEs.[3] In the case of plasmid DNA,[17,22−34] which represents the most biologically significant target, most measurements report a decrease of the intact supercoiled population or the production of single and double strand breaks for thin films of about 10-nm thickness as a function of electron energy under different conditions. In only a few of these[32−34] have attempts been made to measure the *G* values. Yet, even in these measurements, there is no guarantee that the energy of the electrons was completely deposited in the film, so the *G* values might have been

Received: August 17, 2011
Revised: October 12, 2011
Published: October 30, 2011

ACS Publications © 2011 American Chemical Society

underestimated. Hence, there exists a need to develop a method to alleviate this problem so as to derive the best possible G values for LEE-induced damage (G_{LEE}), particularly if one wants to compare the efficiency of LEE damage to biomolecules with that of other particles and photons under various experimental conditions reliably.

Films can be bombarded with two different sources of LEEs: either a direct monochromatic electron beam impinging from a vacuum onto the film surface or photoelectrons emitted from the metal substrate on which the film is deposited. The former source has the advantage of being monoenergetic, whereas the photoelectron source makes it possible to induce LEE damage in biomolecules under gaseous atmospheres at atmospheric pressure (i.e., under conditions closer to those of living cells). Studies of the damage to DNA resulting from the emission of low-energy photoelectrons were introduced by Cai et al. in 2005.[32] The photoelectrons (mean energy of 5.85 eV) were produced by a tantalum surface exposed to Al K_α X-rays of 1.5 keV under a vacuum. The apparatus and the technique were further developed by Brun et al.[33] and Alizadeh et al.[34] to perform experiments at atmospheric temperature and pressure.

In the present article, we report the results of a study of the dependence of LEE-induced DNA damage on average film thickness. We found that, with the apparatus recently developed by Alizadeh et al.,[34] it is possible to explore a much larger range of film thicknesses than in previous experiments. By plotting damage and the corresponding G_{LEE} value as a function of thickness, we obtained more reliable estimates, as well as a factor for correcting the values obtained at too-small thicknesses. A compilation of corrected G values provides solid evidence of the greater efficiency of LEEs to induce DNA damage compared to other types of radiation.

2. EXPERIMENTAL METHODS

In the present experiments, plasmid DNA films were deposited on two different types of substrate: an insulator substrate (glass) and an electron-emitting tantalum substrate. They were prepared by lyophilization with a technique previously described in detail.[34] The films were irradiated with Al K_α X-rays of 1.5 keV. Damage produced on the glass substrate was attributed to energy absorption from X-rays,[32,34] whereas that produced on the metal substrate arose from the absorption of energy from both the soft X-ray beam and the secondary electrons (SEs) emitted from the tantalum surface.[34] From a comparison of the results obtained with DNA films deposited on glass and tantalum, the damage created by LEEs emitted from tantalum was deduced, and the G values were calculated for LEEs under dry N_2 at atmospheric pressure and temperature. Atmospheric-pressure experiments were chosen so as to obtain G values under conditions closer to those used in radiation chemistry measurements.

2.1. Preparation of Plasmid DNA Films. Supercoiled DNA [pGEM-3Zf(−) bacterial plasmid DNA, 3197 base pairs, ca. 1.97×10^6 amu, Promega] was obtained from *Escherichia coli* JM109 host and purified using Qiagen kits. To protect the plasmid DNA from degradation, the DNA pellet was then redissolved in Tris−EDTA (TE) buffer (10 mM Tris, 1 mM EDTA) at pH 8. Prior to use, DNA was cleaned of TE by passing the solution through a homemade microcolumn of Sephadex G-50 resin on a bed of glass beads, to remove the small molecules of salts from the solution.[35,36] The concentration of DNA in the filtered solution was then measured spectrophotometrically from its absorbance at 260 nm, assuming a molar absorption coefficient of 5.3×10^7 L mol^{-1} cm^{-1} at pH 7.0 for DNA.[37] DNA solutions were then diluted in doubly distilled H_2O to obtain the different concentrations of DNA required to make DNA films of variable thicknesses.

A specific volume (V) of a known concentration of plasmid dissolved in nanopure water was spread on clean tantalum and glass surfaces and freeze-dried (lyophilized) at −70 °C under a pressure of 1−3 mTorr for about 2 h. The dried sample had a ring shape of average radius r. Assuming a density of $\rho = 1.71$ g/cm^3 for the plasmid extracted from *E. coli*,[38] the average thicknesses (t) of different groups of DNA films were determined by applying the formula

$$m_{DNA} = \rho V = \rho S t = \rho(\pi r^2)t \quad (1)$$

where m_{DNA} is the mass of DNA in each sample and S is the area of the sample. Thus, by measuring S, it was possible to deduce t, the average thickness of the sample, within a 30% error, which arose principally from the uncertainty in S. The spatial variations in the thickness can be estimated from previous measurements.[3]

Charge accumulation in films prepared by the present technique has been measured by monitoring the energy of the onset of the transmission of electrons through the film from a vacuum to the tantalum substrate.[3] Because a positive energy shift of this onset is caused by electrons trapped in the film, it has been repeatedly possible to estimate that, beyond an average thickness of ∼10 nm, the samples started to charge when impinged by 1−10 eV electrons. For uniform DNA films, this measurement would translate into an electron range on the order of 10 nm. Highly nonuniform samples would charge at a much lower average thickness, as 10-nm regions would be reached with less DNA. The thermalization distance of 10 eV electrons in DNA is 12 ± 1 nm,[39] and that of 1−10 eV electrons in water ice is 11 ± 3 nm on average.[40] Thus, with the present source composed mostly of electrons between 0 and 10 eV (see section 2.4), we expect electrons to be trapped within a distance of 11 ± 3 nm, which corresponds to the onset thickness of charging. Thus, we conclude that the spatial thickness variations in our films cannot be much larger than the errors in the electron thermalization distance (±3 nm) and the average thickness measurements (±3 nm). Thus, according to this estimate, the largest spatial variation of the average thickness of our films should be 60%.

2.2. Experimental Setup and Irradiation Conditions. The 1.5 keV Al K_α X-rays were generated from a cold-cathode source constructed by Alizadeh et al,[41] according to the original design of Hoshi et al.[42] A plasma discharge with a 5.5 mA current is formed between a cathode and an aluminum foil target in a vacuum chamber. Aluminum characteristic K_α X-rays, produced by electron bombardment of the target, travel outside the chamber through a flight tube continuously flushed with helium gas at atmospheric pressure. The X-rays then pass through a thin foil of mylar to enter a small chamber filled by dry N_2 at atmospheric pressure, where plasmid DNA films are deposited on the different substrates.

The freeze-dried films are transferred to the X-ray apparatus for exposure to X-rays of varying fluence, in the presence of nitrogen gas having a stated purity of 99.9% and no humidity, as monitored by a hygrometer sensor placed in the irradiation chamber. For each group of samples, two samples were used as controls; that is, these samples were lyophilized, kept under the

same atmospheric experimental conditions as the irradiated samples, and recovered, but not irradiated by X-rays.

2.3. Quantification of the Yields by Agarose Gel Electrophoresis. After irradiation, the samples were immediately retrieved from the chamber and the tantalum and glass surfaces with 95−98% efficiency by dissolving them in TE buffer. The fractions of various forms induced in DNA by irradiation was then determined by a 1% agarose gel electrophoresis run in Tris Acetate−EDTA (TAE) buffer (40 mM Tris acetate, 1 mM EDTA, pH 8.0) at 10 V cm^{-1} for 7 min and 7.5 V cm^{-1} for 68 min. The relative proportion of each configuration was expressed as a percentage of the total amount. The undamaged plasmid exists in a supercoiled (SC) topological form. Induction of an SSB converts the plasmid into a relaxed form or "nicked circular" (C) form, whereas induction of a double strand break (DSB) within both the SC and C forms changes the plasmid into its linear (L) form. In the present study, before irradiation, 96% of the extracted plasmid was in the supercoiled form, and the rest was in the relaxed circular (C, > 3%) and concatemeric (CM, < 1%) configurations.

About 100 ng of DNA from each recovered solution was prestained with 3 μL of 100× SYBR Green I (Molecular Probes) for loading in each well. The samples were incubated with SYBR Green I for at least 15 min prior to electrophoresis. The gel itself was stained with 8 μL of 10000× concentration SYBR Green I. After electrophoresis, the gels were scanned with a Typhoon-Trio laser scanner (GE Healthcare) using the blue fluorescence mode at an excitation wavelength of 488 nm and filter type 520 BP 40. Various DNA forms were quantified using ImageQuant software (Molecular Dynamics). These values were corrected using a normalization factor, because of the weaker binding of SYBR Green I to the supercoiled form of DNA compared to the nicked circular and linear configurations. For the pGEM-3Zf(−) plasmids used in this work, a correction factor of 1.4 was determined after quantification by ImageQuant.

The number of X-ray photons incident on the samples was determined within an accuracy of 8% using GAFCHROMIC HD-810 dosimeter films. A detailed description of the calculations and the calibration of the sensitivity of the films can be found in ref 34.

2.4. SE Emission from Tantalum. X-ray photons interacting with metal atoms produce energetic photoelectrons and Auger electrons inside the metal (mainly through the photoelectric effect). These electrons lose energy, producing a distribution at the surface of the tantalum substrate consisting essentially of LEEs. The SE energy distribution curve from a tantalum substrate has been given in our previous work.[34] The electron energy distribution peaks at 1.4 eV and 95% of the electrons have energies below 30 eV. The average energy is 5.85 eV. A total electron yield of 0.049 electron per photon is obtained from this distribution.[34] The current of the X-ray-induced SEs emitted from the tantalum surface was measured to be 0.17 ± 0.02 nA. Consequently, the electron flux and the quantum yield of electron emission were calculated to be (0.54 ± 0.2) × 10^9 electrons s^{-1} cm^{-2} and 0.047 ± 0.005 electron per photon, respectively. The latter was used in G value calculations as η_e, the number of SEs induced per photon entering the tantalum substrate.

2.5. Calculation of *G* values. The molecular weight of plasmid DNA and its mass attenuation coefficient for 1.5 keV X-rays were calculated to be $M_W = 2.25 \times 10^6$ g/mol and μ/ρ = 1056 cm^2/g, respectively, based on the DNA's composition and μ/ρ of individual atoms.[43] For each thickness, the dose−response curves (i.e., percentage loss of SC DNA as a function of incident photon fluence) for both glass and tantalum substrates were plotted from zero fluence to 25 × 10^{11} photons/cm^2. Each of these dose responses curves required measurements on 3 samples at each dose for six different doses for a total of almost 360 analyses of DNA damage by agarose gel electrophoresis. The slopes of the linear-least-squares fits of respective exposure curves represent the yields of damages induced at each film thickness. Thus, the number of damaged DNA molecules induced in each film for a given photon fluence (Φ) is given by $D_{Gl} = |\Delta SC_{Gl}|\Phi N_{DNA}$ and $D_{Ta} = |\Delta SC_{Ta}|\Phi N_{DNA}$, where N_{DNA} is the number of DNA molecules in each sample and $|\Delta SC_{Gl}|$ and $|\Delta SC_{Ta}|$ are the slopes of the dose−response curves for films deposited on glass and tantalum, respectively. The number of absorbed photons in the DNA film can be calculated as

$$X_{Abs} = \Phi S\left[1 - \exp\left(-\frac{\mu}{\rho}\right)\rho t\right] \quad (2)$$

and the number of photons passing through the film to produce photoelectrons at the tantalum substrate as

$$X_{Trans} = \Phi S\left[\exp\left(-\frac{\mu}{\rho}\right)\rho t\right] \quad (3)$$

In radiation chemistry, the G value is commonly expressed in two different units, D/100 eV and nanomoles (or micromoles) per joule, where D represents one damaged molecule and 1 D/100 eV = 103 nmol/J. Thus, from our results, G_{LEE} is given by

$$G_{LEE} = \frac{(D_{Ta} - D_{Gl})}{\eta_e X_{Trans}(5.85\ \text{eV})} \times 100\ \text{eV} \quad (4)$$

Equation 4 gives G values in D/100 eV.

3. RESULTS AND DISCUSSION

For the thinnest DNA films in our experiments (~2 nm), only >0.1% of the incident X-ray photon flux interacted directly with DNA molecules, whereas 99.9% passed through the DNA film to the tantalum substrate where they induced SEs from the metal surface. For the thickest film in this work (~200 nm), we estimate that almost 4% of the incident photons were absorbed within the DNA (i.e., 96% reached the substrate). Figure 1 shows the dependence of the number of absorbed photons on the thickness of the DNA film for an incident fluence of 10^{12} photons/cm^2, calculated from eq 2. The error bars reflect the deviations in the measurements of the photon flux and the thickness or area of the films. X-ray absorption obeys the Beer−Lambert law and should have an exponential behavior. However, within experimental errors, the absorption of the X-rays in DNA films can be considered to increase linearly with thicknesses below 250 nm. Consequently, the number of damaged DNA molecules with film thickness was fitted to a linear function.

Figure 2 presents the variation in the number of damaged molecules as a function of DNA film thickness. As expected, for the same thickness, the number of damaged DNA molecules for plasmid deposited on tantalum substrates (i.e., damage induced by both soft X-rays and LEEs) was greater than that for DNA deposited on glass (i.e., damage arising from soft X-rays). The points recorded above 200 nm in Figure 2a, which do not obey the previously mentioned linearity, show the limitations of the

instrument. Beyond 150 nm, the films cannot be grown to a size that fits completely under the area of the X-ray beam.

As previously explained, DNA films deposited on tantalum were irradiated to measure the additional damage induced by photoemitted LEEs. Because the latter have a very short effective range,[4] there was no reason to continue measurements beyond 80 nm (Figure 2b). This is clearly shown in Figure 3. The curve of Figure 3 illustrates the contribution to DNA damage induced by X-rays and LEEs at different film thicknesses through an enhancement factor (EF). The EF values were derived by dividing the yield of damaged DNA on the tantalum substrate by that measured in DNA films on glass, under the same experimental conditions. As presented in Figure 3, for the thinnest film in our experiments, this factor was almost 1.6, agreeing well with the results of Cai et al.[32] (i.e., 1.5 in monolayer films). Thus, in thinner films, the photoemitted LEEs significantly increased DNA damage, considering that only 47 ± 5 photoelectrons escaped the surface per thousand incident photons. With increased thickness, the EFs approached unity, indicating a lesser relative contribution of LEEs to the damage, owing to the increased absorption of X-ray photons by an increasing the amount of DNA molecules.

Calculated G values for loss of SC DNA by LEEs (G_{LEE}) under N_2 atmosphere are shown as a function of DNA film thickness in Figure 4. The solid curve is a saturating exponential fitted to the data. G_{LEE} was found to rise rapidly as a function of thickness until saturating at 260 ± 50 nmol/J around 20 ± 6 nm. As expected, this behavior indicates that, below 20 nm, a fraction of SEs escaped from the DNA film into vacuum without depositing all of their energy. For t > 20 nm, all of the SEs seemed to remain in the film and deposit their energy. In other words, sufficient material covered the tantalum substrate to absorb all of the electrons. As discussed in section 2.1, the thermalization distance of most photoelectrons emanating from the tantalum surface was estimated to be 11 ± 3 nm. Thus, a film of 20-nm average

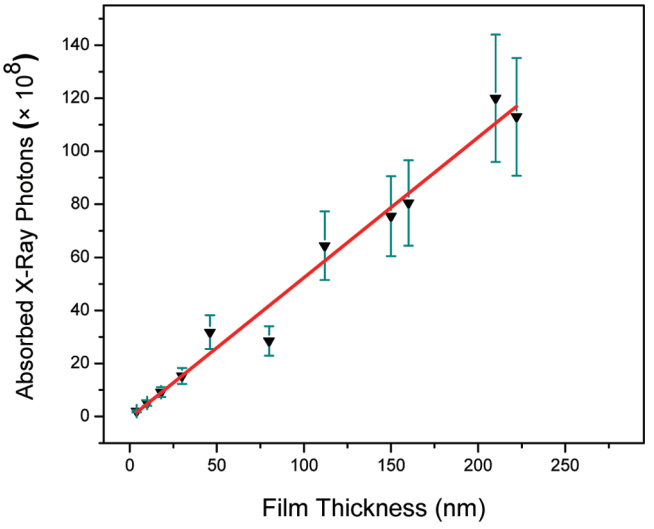

Figure 1. Number of absorbed X-ray photons as a function of DNA film thickness for an incident fluence of 10^{12} photons/cm^2.

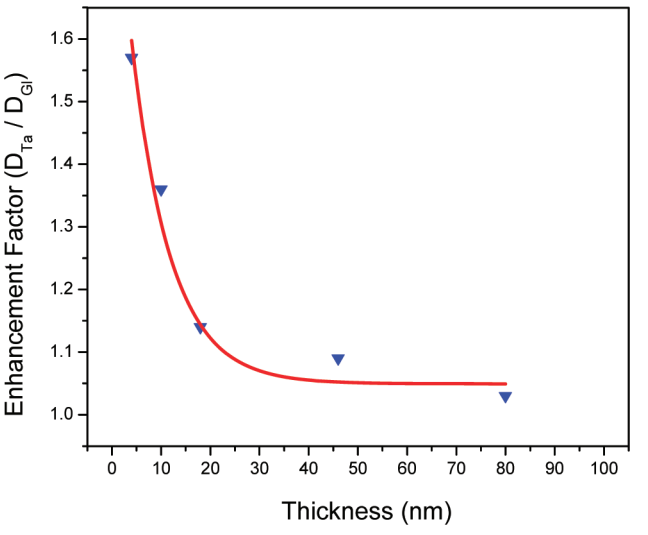

Figure 3. Dependence of the enhancement factor (EF) as an exponentially decaying function of the DNA film thickness. The EF is derived by dividing the yield of damaged DNA on the tantalum substrate by that measured in DNA films on glass, under the same experimental conditions.

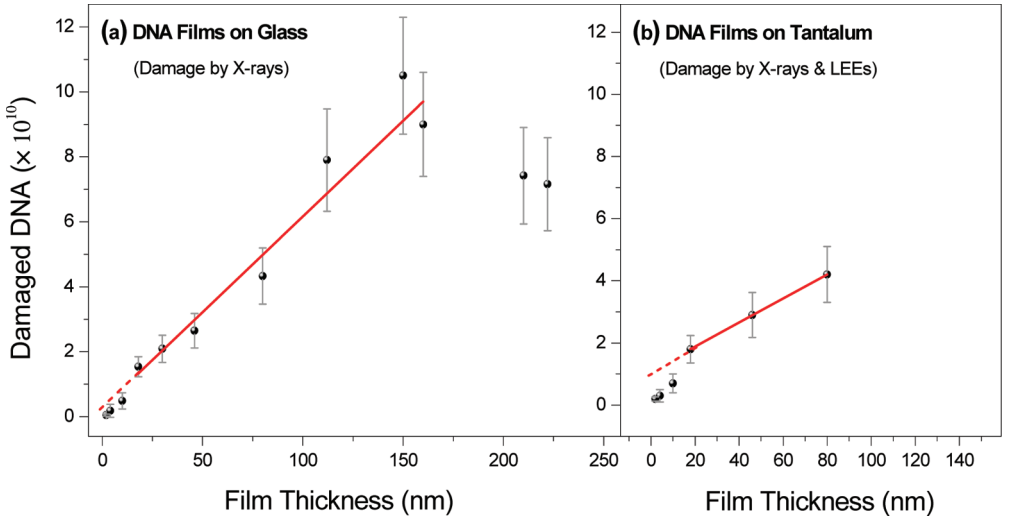

Figure 2. Number of damaged DNA molecules in a film for samples deposited on (a) glass and (b) tantalum as a function of DNA film thickness for an incident fluence of 10^{12} photons/cm^2.

dx.doi.org/10.1021/jp207922n |J. Phys. Chem. B 2011, 115, 14852–14858

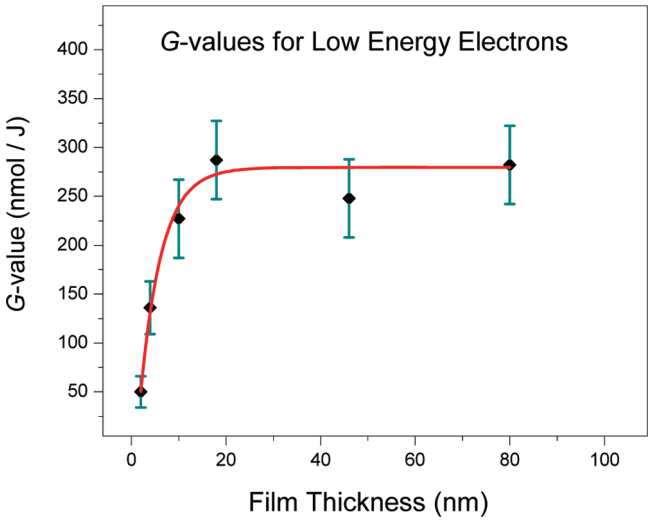

Figure 4. *G* values for the loss of the SC configuration of DNA induced by LEEs under a N_2 atmosphere as a function of film thickness.

Table 1. G_{LEE} for the Loss of SC DNA Obtained by Various Authors, under Different Conditions, Along with the Corrected *G* Values Deduced from eq 5 [a]

ref	atmosphere	film thickness (nm)	G_{LEE} (nmol/J)	G_P (nmol/J)
Alizadeh et al.[34]	N_2	10	227 ± 15	260 ± 50
Alizadeh et al.[34]	O_2	10	415 ± 15	477 ± 38
Alizadeh et al.[44]	N_2O	10	737 ± 15	847 ± 67
Brun et al.[33]	vacuum	10	400 ± 200	460 ± 230
Brun et al.[33]	air	10	600 ± 200	690 ± 230
Cai et al.[32]	vacuum	2	50 ± 16	295 ± 94

[a] Extent of hydration is expressed in terms of moles of water per mole of nucleotides, represented by Γ. For freeze-dried DNA samples, Γ is considered to be 2.5 and for hydrated DNA 15 < Γ< 35[13] (see Table 2). All data in this table were recorded with Γ = 2.5, with the exception of those obtained in air at Γ = 20.[33]

thickness has spatial variations in thickness from 11 ± 3 nm to an upper bound that cannot be deduced from the data. Assuming that spatial variations were uniformly distributed around the mean thickness, the local thickness varied from 11 to 29 nm along the plane of the tantalum substrate. These fluctuations correspond to a maximum variation of 45% of the mean thickness. They are smaller than those predicted from charge measurements in section 2.1 (i.e., 60%), but if we include the error in the thermalization distance of the electrons, the values are similar. These fluctuations are large, but fortunately, at and beyond a thickness of 20 nm, the *G* values became independent of nonuniformity, because the electrons deposited all of their energy in the film. Consequently, as the film thickness increased, the *G* value remained constant. Thus, the present method allows for the determination of *G* values that are independent of spatial film irregularities. This is a considerable asset considering the difficulties in producing uniform DNA films.

We note, however, that some electrons are expected to scatter back into the metal substrate without losing all of their energy in the film for both thick and thin films. Thus, even though the saturation of the curve in Figure 4 provides the most valid *G* value, it still underestimates the real G_{LEE} value. Undoubtedly, at thicknesses of 10−80 nm, the film must be charging from electrons that thermalize, because in DNA the effective range of LEEs is about 11 nm.[23] However, within our experimental error, it seems that charging, which should increase considerably from 10 to 80 nm, does not modify the smooth exponentially saturating behavior of the curve of Figure 4. This observation and the preceeding discussion of film uniformity lend credibility to the present experiments as a reliable method for obtaining the best possible *G* values for LEEs.

Knowledge of the G_{LEE} value in the plateau allows for the calculation of a factor to find the difference between the most reliable *G* value and the one measured at thicknesses that are too small. This factor is calculated as

$$f = \frac{G_P - G_t}{G_P} \quad (5)$$

where f is the fraction of actual damage induced in films of thickness (t) that was caused by escaping electrons and G_P and G_t

Table 2. *G* Values for the Formation of SSB in DNA by Different Types of Radiation under Various Experimental Conditions

ref	radiation	experimental conditions	*G* value (nmol/J)
Ito et al.[13]	^{60}Co γ-rays (1.17 MeV)	dry DNA	56
		hydrated DNA	120
Yokoya et al.[48]	^{60}Co γ-rays	dry DNA	54 ± 9
		hydrated DNA	72 ± 5
Yokoya et al.[49]	α-particles (3.31 MeV)	dry DNA	48 ± 4
		hydrated DNA	60 ± 9
Purkayastha et al.[45]	X-rays (70 keV)	dry DNA	69 ± 14
		hydrated DNA	54 ± 7
Cai et al.[32]	Al K_α X-rays (1486 eV)	dry DNA	57 ± 1
Cai et al.[47]	Al K_α X-rays	dry DNA (20 mm^2)	62 ± 6
Yokoya et al.[46]	soft X-rays (2153 eV)	dry DNA	43 ± 10
		hydrated DNA	110 ± 12
Brun et al.[33]	Al K_α X-rays	dry DNA	44 ± 6
Brun et al.[33]	Al K_α X-rays	dry DNA	42 ± 6
Alizadeh et al.[41]	Al K_α X-rays	dry DNA (N_2)	60 ± 4
Alizadeh et al.[41]	Al K_α X-rays	dry DNA (O_2)	117 ± 8
Alizadeh et al.[44]	Al K_α X-rays	dry DNA (N_2O)	92 ± 13

are the G values measured at the plateau and at thickness t, respectively. In Table 1, we list G_{LEE} values obtained under different conditions, previously recorded with the same apparatus,[32−34,44] along with the corrected G values deduced from Figure 4 or from eq 4, that is , $G_P = G_t/(1 - f)$. We can also consider CF = $1/(1 - f)$ as a correction factor for finding G_P for LEEs under different environmental conditions for each specific thickness. For instance, for films of 10- and 2-nm average thicknesses, the CFs are 5.9 ± 0.7 and 1.15 ± 0.03, respectively, which correspond to 83% and 13% corrections in G_{LEE} for 2- and 10-nm films. This indicates that, for thinner films, the calculated G value is much lower than the G_P value obtained in this work (i.e., more LEEs escape from thinner films).

Owing to the universality of G value, we are now in a position to compare the efficiency of LEEs to damage biomolecules with that of other types of radiation under various environmental conditions. Such G values are presented in Table 2 for the formation of SSBs. As already reported in many studies and listed in Table 2, X- and γ-rays of varying energies induce damage in DNA under dilute aqueous solution, hydrated, and dry conditions. Most of the results in this table are in good agreement with each other, such as those of Purkayastha et al.,[45] Yokoya et al.,[46] and Cai et al.[32,47] for dry DNA.

Because the formation of SSBs is the main type of damage induced by LEEs for the data of Table 1, G_{LEE} for loss of SC DNA can be compared to G values for SSB damage mentioned in Table 2. Thus, these two tables provide the most reliable comparison of G_{LEE} for DNA with those for other types of radiations. They show that G values for LEEs are higher than those for photons and even high-linear-energy-transfer radiation such as α-particles under different conditions. LEEs were found to have higher effectiveness in causing damage to DNA relative to higher-energy radiation. The reasons for this higher effectiveness have been discussed in previous publications.[32−34]

4. CONCLUSIONS

G values for the loss of supercoiled DNA induced by LEEs with an energy distribution peaking around 1.4 eV were determined in DNA films of thicknesses ranging from ∼2 to 80 nm. We found that the number of damaged DNA molecules and the G values for LEEs increased with average sample thickness until saturation was observed around 20 nm. Although LEEs have an effective range of the order of 10 nm, we found that, for thicknesses of <20 nm, some of them escape into the surrounding atmosphere without depositing all of their energy in the DNA film. Thus, the calculated G values in such thin films are underestimated, if one assumes that all of the energy of the interacting electrons is absorbed in the DNA layers. In this work, we presented a method to obtain more reliable G values for LEE-induced damage to DNA that are independent of film thickness and its spatial variation. Thus, the method allows for the determination of reliable G_{LEE} values even if the spatial distribution of DNA in the irradiated sample is highly irregular. It also allows for the correction of previous determinations of G_{LEE} values measured in too-thin films. From those corrected values, the first comparison of G_{LEE} values obtained under various experimental conditions was made with those for DNA damage induced by other types of radiation.

AUTHOR INFORMATION

Corresponding Author

*E-mail: Elahe.Alizadeh@USherbrooke.ca. Phone: +1 819 346 1110 (15863). Fax: +1 819 564 5442.

ACKNOWLEDGMENT

This work was funded by the Canadian Institutes of Health Research (CIHR) and the Marie Curie Incoming International Fellowship program. The authors thank Dr. A. D. Bass and M. Rezaee for their comments. Thanks are also extended to P. Cloutier and S. Girouard for technical support and preparation of plasmid DNA.

REFERENCES

(1) Von Sonntag, C. *The Chemical Basis of Radiation Biology*, 1st ed.; Taylor and Francis: London, 1987.
(2) Horan, A. D.; Giandomenico, A. R.; Koch, C. J. *Radiat. Res.* **1999**, *152*, 144–153.
(3) Sanche, L. In *Radical and Radical Ion Reactivity in Nucleic Acid Chemistry*; Greenberg, M. M., Ed.; John Wiley and Sons: New York, 2009; pp 239−293.
(4) Nikjoo, H.; Lindborg, L. *Phys. Med. Biol.* **2010**, *55*, R65–R109.
(5) Goodhead, D. T. *Can. J. Phys.* **1989**, *68*, 872–886.
(6) Chatterjee, A.; Magee, J. L. In *Radiation Chemistry: Principles and Applications*; Farhataziz, Rodgers, M. A. J., Eds.; VCH Publishers: New York, 1987; pp 173−199.
(7) Olive, P. L. *Radiat. Res. (Suppl.)* **1998**, *150*, 42–51.
(8) Spotheim-Maurizot, M.; Mostafavi, M.; Douki, T.; Belloni, J. *Radiation Chemistry*; EDP Sciences: Paris, 2008.
(9) Folkard, M.; Prise, K. M.; Turner, C. J.; Micheal, B. D. *Radiat. Prot. Dosim.* **2002**, *99*, 147–149.
(10) Wang, C. R.; Nguyen, J.; Lu, Q. B. *J. Am. Chem. Soc.* **2009**, *131*, 11320–11322.
(11) Sanche, L. *Nature* **2009**, *461*, 358–359.
(12) Fricke, H.; Hart, E. J. In *Radiation Dosimetry*, Attix, F. H., Roesch, W. C., Academic Press: New York, 1966; Vol. II.
(13) Ito, T.; Baker, S. C.; Stickley, C. D.; Peak, J. G.; Peak, M. J. *Int. J. Radiat. Biol.* **1993**, *63*, 289–296.
(14) Collinson, E.; Dainton, F. S.; Kroh, J. *Proc. R. Soc. London, Ser. A* **1962**, *265*, 407–421.
(15) Gordon, S.; Hart, E. J. *Radiat. Res.* **1961**, *15*, 440–451.
(16) Fregene, A. O. *Radiat. Res.* **1967**, *31*, 256–273.
(17) Boudaïffa, B.; Cloutier, P.; Hunting, D.; Huels, M. A.; Sanche, L. *Science* **2000**, *287*, 1658–1660.
(18) Barrios, R.; Skurski, P.; Simons, J. *J. Phys. Chem. B* **2002**, *106*, 7991–7994.
(19) Pimblott, S. M.; LaVerne, J. A. *Radiat. Phys. Chem.* **2007**, *76*, 1244–1247.
(20) Goodhead, D. T.; Nikjoo, H. *Radiat. Prot. Dosim.* **1990**, *3*, 343–350.
(21) Arumainayagam, C. R.; Lee, H.; Nelson, R. B.; Haines, D. R.; Gunawardane, R. P. *Surf. Sci. Rep.* **2010**, *65*, 1–44.
(22) Folkard, M.; Prise, K. M.; Vojnovic, B.; Davies, S.; Roper, M. J.; Michael, B. D. *Int. J. Radiat. Biol.* **1993**, *64*, 651–658.
(23) Panajotovic, R.; Martin, F.; Cloutier, P.; Hunting, D.; Sanche, L. *Radiat. Res.* **2006**, *165*, 452–459.
(24) Zheng, Y.; Hunting, D.; Ayotte, P.; Sanche, L. *Phys. Rev. Lett.* **2008**, *100*, 198101–198105.
(25) Chen, Y.; Aleksandrov, A.; Orlando, T. M. *Int. J. Mass Spectrom.* **2008**, *277*, 314–320.
(26) Dumont, A.; Zheng, Y.; Hunting, D.; Sanche, L. *J. Chem. Phys.* **2010**, *132*, 045102.
(27) Grieves, G. A.; McLain, J. L.; Orlando, T. M. In *Charged Particle and Photon Interaction with Matter: Recent Advances, Applications, and Interfaces*; Hatano, Y., Katsumura, Y., Mozumder, A. M., Eds.; CRC Press: Boca Raton, FL, 2011; Chapter 18, pp 473−502.
(28) Martin, F.; Burrow, P. D.; Cai, Z.; Cloutier, P.; Hunting, D.; Sanche, L. *Phys. Rev. Lett.* **2004**, *93*, 068101–1−4.
(29) Orlando, T. M.; Oh, D.; Chen, Y.; Aleksandrov, A. B. *J. Chem. Phys.* **2008**, *128*, 195102.

(30) Huels, M. A.; Boudaïffa, B.; Cloutier, P.; Hunting, D.; Sanche, L. *J. Am. Chem. Soc.* **2003**, *125*, 4467–4477.
(31) Solomun, T.; Seitz, H.; Sturm, H. *J. Phys. Chem. B* **2009**, *113*, 11557–11559.
(32) Cai, Z.; Cloutier, P.; Hunting, D.; Sanche, L. *J. Phys. Chem. B* **2005**, *109*, 4796–4800.
(33) Brun, É.; Cloutier, P.; Sicard-Roselli, C.; Fromm, M.; Sanche, L. *J. Phys. Chem. B* **2009**, *113*, 10008–10013.
(34) Alizadeh, E.; Cloutier, P.; Hunting, D.; Sanche, L. *J. Phys. Chem. B* **2011**, *115*, 4523–4531.
(35) Sambrook, R. *Molecular Cloning, A Laboratory Manual*; Cold Spring Harbor Laboratory Press: New York, 2001.
(36) Cecchini, S.; Girouard, S.; Huels, M. A.; Sanche, L.; Hunting, D. *Radiat. Res.* **2004**, *162*, 604–615.
(37) Manchester, K. L. *Biotechniques* **1996**, *20*, 968–970.
(38) Adams, R. L. P.; Knowler, T.; Leader, D. P. *The Biochemistry of the Nucleic Acids*, 10th ed.; Chapman and Hall: London, 1986.
(39) Boudaïffa, B.; Cloutier, P.; Hunting, D.; Huels, M. A.; Sanche, L. *Radiat. Res.* **2002**, *157*, 227–234.
(40) Meesungnoen, J.; Jay-Gerin, J. P.; Filali-Mouhim, A.; Mankhetkorn, S. *Radiat. Res.* **2002**, *158*, 657–660.
(41) Alizadeh, E.; Cloutier, P.; Sanche, L. In *Proceedings of the 2nd International Conference on Nanotechnology: Fundamentals and Applications*; International ASET: Ottawa, ON, Canada, 2011; Vol. 192, pp 1−8.
(42) Hoshi, M.; Goodhead, D. T.; Brenner, D. J.; Bance, D. A.; Chmielewski, J. J.; Paciotti, M. A.; Bradbur, J. N. *Phys. Med. Biol.* **1985**, *30*, 1029–1041.
(43) Hubbell, J. H.; Seltzer, S. M. X-ray Mass Attenuation Coefficients. In *NIST Chemistry WebBook*; NIST Standard Reference Database Number 126; National Institute of Standards & Technology: Gaithersburg, MD, http://physics.nist.gov/PhysRefData/XrayMassCoef/ (accessed July 2004).
(44) Alizadeh, E.; Sanche, L. *Radiat. Phys. Chem.* **2012**, *81*, 33–39.
(45) Purkayastha, S.; Milligan, J. R.; Bernhard, W. A. *J. Phys. Chem. B* **2006**, *110*, 26286–26291.
(46) Yokoya, A.; Cunniffe, S. M. T.; Watanabe, R.; Kobayashi, K.; O'Neill, P. *Radiat. Res.* **2009**, *172*, 296–305.
(47) Cai, Z.; Cloutier, P.; Sanche, L.; Hunting, D. *Radiat. Res.* **2005**, *164*, 173–179.
(48) Yokoya, A.; Cunniffe, S. M. T.; O'Neill, P. *J. Am. Chem. Soc.* **2002**, *124*, 8859–8866.
(49) Yokoya, A.; Cunniffe, S. M. T.; Stevens, D. L.; O'Neill, P. *J. Phys. Chem. B* **2003**, *107*, 832–837.